High-Resolution Quadrature Photopyroelectric Spectroscopy of *a*-Si:H Thin Films Deposited on Silicon Wafers

JUN SHEN, ANDREAS MANDELIS,* ANDREAS OTHONOS, and JOSEPH VANNIASINKAM

Photothermal and Optoelectronic Diagnostics Laboratory, Department of Mechanical Engineering, University of Toronto, Toronto, M5S 1A4, Canada (J.S., A.M., J.V.); and Ontario Laser and Lightwave Research Center, University of Toronto, Toronto, M5S 1A4, Canada (A.O.)

The recently developed photothermal technique of quadrature photopyroelectric spectroscopy (Q-PPES) has been applied to measurements of amorphous Si thin films deposited on crystalline Si substrates. Direct, meaningful comparisons have been made between purely optical transmission in-phase (IP-PPES) spectra, and purely thermal-wave sub-gap spectra with the use of a novel noncontacting PPES instrument to record lock-in in-phase and quadrature spectra, respectively. FT-IR transmission spectra have also been obtained for a comparison with this IP-PPES optical method. The results of the present work showed that the FT-IR method performs the worst in terms of spectral resolution of thin films and sub-bandgap defect/impurity absorptions inherent in the Si wafer substrate. The optical IP-PPES channel, however, albeit more sensitive than the FT-IR technique, fails to resolve spectra from surface films thinner than 2100 Å, but is sensitive to sub-bandgap absorptions. The thermal-wave Q-PPES channel is capable of resolving thin-film spectra well below 500 Å thick and exhibits strong signal levels from the crystalline Si sub-bandgap absorptions. Depending on the surface thin-film orientation toward, or away from, the direction of the incident radiation, the estimated minimum mean film thickness resolvable spectroscopically by Q-PPES is either 40 Å or 100 Å, respectively.

Index Headings: **Phytopyroelectric spectroscopy (PPES); Quadrature-PPES; Amorphous hydrogenated silicon thin films; FT-IR spectroscopy.**

INTRODUCTION

In recent years photopyroelectric spectroscopy (PPES) has been used successfully for the characterization of thin semiconducting films. Mandelis et al.[1] first performed PPES measurements of an *a*-Si:H thin film on quartz. Christofides et al.[2,3] have extended the use of PPES to spectroscopic measurements of thick crystalline Ge and Si wafer substrates. By considering the phase of the lock-in amplifier PPES signal and placing the sample in contact with the active sensor element (polyvinylidene fluoride, PVDF) of the spectrometer, it has become possible to obtain sub-gap spectra of amorphous silicon thin films deposited on crystalline silicon at an instrumental sensitivity limit of $\beta t = 5 \times 10^{-3}$ (β: optical absorption coefficient; t: film thickness).[4] Early on, it was recognized in this laboratory that a potentially limiting feature of PPES sensitivity was the usually uncontrollable thermal resistance between the contacting sample and the flat surface of the PVDF element. Recent detailed simulations of the effects of interfacial thermal resistances, including that of spray-painted black layers on the PVDF surface for purposes of signal enhancement, have been able to deconvolute the spectral information from ultrathin quantum-well structures on GaAs substrates.[5] The price of this deconvolution is the theoretical simulation complexity, which is accompanied by some degree of irreproducibility with each new sample–detector contact. As a consequence, the sensitivity, spectral resolution, and maximum dynamic range of the technique can be compromised under very low signal conditions. Nevertheless, the *inherently high* dynamic range of PPES has enabled us,[1] and others,[6,7] to probe sub-gap regions in hydrogenated amorphous silicon films with a sensitivity of $\beta t \sim 10^{-3}$. Coufal[8] measured PPE phase shifts in the 0.1–0.9° range with his fixed-thickness, contacting, thermal-wave phase shifter with ~0.1° phase resolution. Recent instrumental developments on our original PPE spectrometer[9] have allowed the elimination of contact thermal resistance and are centered on the quadrature signal channel as the optimally sensitive spectroscopic mode. In comparison with Coufal's method, Q-PPES detection using an absorption-free, highly controllable, variable-thickness, thermal-wave phase shifter (i.e., the sample backing airgap layer) allowed the measurement of minute signals corresponding to phase shifts in the 0.02–0.2° range with 0.015° phase resolution when used with transparent optical materials, specifically with Ti:Sapphire laser rods either spectroscopically[9] or in the scanning imaging mode.[10]

In this work, the recently developed noncontacting PPE thermal-wave phase-shift spectrometer was used to show that sub-gap spectra of *a*-SI:H thin films on silicon can be obtained very reproducibly with a potential thickness resolution down to 40 Å.

THEORETICAL BACKGROUND

The full theoretical treatment of the IP- and Q-PPES signal response from bulk-absorbing solids with a separate surface layer of absorptance $A(\lambda)$ has been presented in Ref. 11. In this brief section, the salient features of the theory will be outlined in order to provide a basis for the interpretation of the observed PPE spectra. Assuming a bulk absorption coefficient $\beta(\lambda)$, surface and bulk optical-to-thermal energy conversion (nonradiative) efficiencies η^s and η^b, respectively, and reflectance $R(\lambda)$, the solution to the thermal-wave equations in the gas (air) and in the solid (s), subject to optical excitation of intensity, I_0, and boundary conditions of temperature and heat-flux continuity, gives the PPE signal response.[11]

Received 24 October 1994; accepted 24 February 1995.
* Author to whom correspondence should be sent.

0003-7028/95/4906-0819$2.00/0

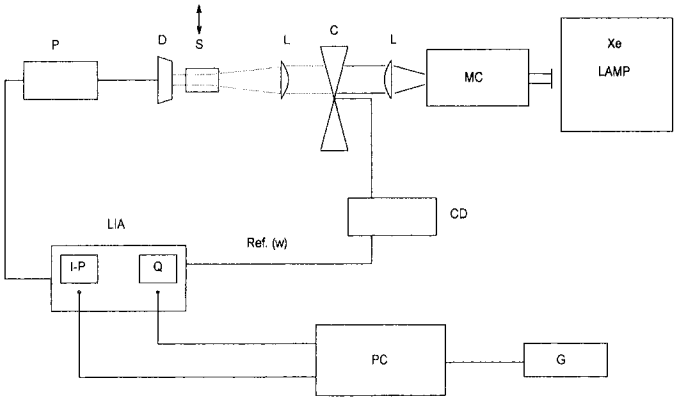

FIG. 1. Schematic diagram of noncontact PPES spectrometer. **MC**, monochromator; **L**, lens; **C**, chopper; **S**, sample with adjustable-positioning micrometer stages with respect to the stationary detector **D**; **D**, PVDF detector assembly; **P**, preamplifier with adjustable bandpass filters; **LIA**, lock-in amplifier (EG&G Model 5210 in IP and Q mode); **CD**, chopper driver; **PC**, computer for data acquisition, processing and analysis; **G**, graphics and plotter.

$$V_L(\omega, \lambda) = S(\omega)C_L(\omega, \lambda) \quad (1)$$

where $S(\omega)$ is an instrumental factor, dependent on PVDF thermophysical properties, among other parameters, and on the angular modulation frequency ω of the exciting optical beam intensity. $S(\omega)$ can be easily normalized out experimentally when all spectroscopy is carried out at a fixed ω. The factor $C_L(\omega, \lambda)$ contains all physical and spectroscopic information (Ref. 11, equation 11) and depends on η^s, η^b, $\beta(\lambda)$, $A(\lambda)$, $R(\lambda)$, sample thickness ℓ, and sample-to-detector distance L.

In the *optical transmission mode* ($L \rightarrow \infty$), the expression for $C_L(\omega, \lambda)$ becomes very simple after normalization with the PPE signal in the absence of the sample layer L. In this case, the normalized PPE signal is given by

$$V_\infty(\lambda, \omega) = \frac{C_\infty(\lambda, \omega)}{C_R(\lambda, \omega)} = \frac{(1 - R)^2}{1 - R^2 e^{-2(\beta l + A)}} e^{-(\beta l + A)} \quad (2)$$

where C_R is the reference PPE signal in the absence of a solid sample layer. The expression, Eq. 2, is purely optical and has no imaginary (thermal-wave) component. Under typical experimental conditions, such as those of the present spectroscopic measurements, the IP-PPES signal at sample–to–detector distance $L \gg \mu_{air}(\omega)$ (μ_{air}: thermal diffusion length in air at the frequency of operation[12]), i.e., at thermally "infinite" sample–detector distance, is given by Eq. 2. Operationally, the conditions of applicability of Eq. 2 to the experimental system of Fig. 1 can be met by separating sample and detector by a "large" distance (~ 1–2 cm) and zeroing the lock-in quadrature, thus allowing the entire transmission signal to appear in the IP channel.

In the *thermal-wave transmission mode* [$L \leq \mu_{air}(\omega)$], C_L can be separated out into three additive components[11] as follows: (1) For optically thin samples,[12] a contribution to the thermal-wave field in the coupling gas (air) from the surface heating of the PVDF detector itself due to the transmitted portion of the exciting radiation through the thickness l of the sample; this term is absent from optically opaque materials. (2) A sample-bulk thermal-wave contribution term due to heat released by the (Si) substrate following intrinsic super-bandgap optical absorption, or extrinsic optical absorption due to sub-bandgap defect structures in the crystal, and optical-to-thermal energy conversion; therefore, this component of the PPES signal is proportional to $\eta^b(\lambda)$. (3) A contribution to the thermal-wave field from the absorbing surface layer of absorptance $A(\lambda)$; this component is proportional to $\eta^s(\lambda)$:

$$V_L(\lambda, \omega) = \frac{C_L(\lambda, \omega)}{C_R(\lambda, \omega)} \propto F_t + \eta^b(\lambda)F_b + \eta^s(\lambda)F_s \quad (3)$$

where the functions F_t, F_b, and F_s are complicated complex functions of the transmitted, bulk, and surface components, respectively (Ref. 11, equation 11). Therefore, they allow for the separation of in-phase and quadrature components by taking $\mathrm{Re}[V_L(\lambda, \omega)]$ and $\mathrm{Im}[V_L(\lambda, \omega)]$, respectively. From the structure of Eq. 3 it turns out that the real part of F_t includes the direct optical transmission component, which is much higher than the imaginary part, typically by 1–2 orders of magnitude, and usually strongly dominates the PPES signal.[10] Thus the major advantage of Q-PPES detection can be understood in terms of the efficient lock-in Q-channel suppression of the real part of the signal dominating component F_t, and the proportional enhancement of the importance of the rest of the components of Eq. 3 in determining the sensitivity of the Q-PPES technique to minute thermal-wave occlusions from bulk and surface. The components F_s and F_b can be calculated numerically once the various parameters of the PPE system are known. These include individual knowledge of the optical absorptances $\beta(\lambda)\ell$ and $A(\lambda)$, the *sum* of which can be found from the IP-PPE experiments reported in this work, but *not* the individual contributions. For this deconvolution to be made, pairs of samples with identical surface absorptances and bulk absorption coefficients and different thicknesses are required.[11] Owing to the unavailability of such samples in this work, the experimental results have been discussed only qualitatively, by necessity.

EXPERIMENTAL

The noncontact PPES spectrometer has been described elsewhere.[9,10] The schematic diagram of the apparatus is shown in Fig. 1. Briefly, the important feature of the spectrometer is the incorporation of a variable-thickness air layer between sample back surface and PVDF pyroelectric detector, acting as a photothermal phase shifter, as a PVDF dc drift compensator, and as a thermal contact resistance eliminator. Optical transmission spectra from *a*-Si:H wafer samples were obtained photopyroelectrically in the purely optical transmission mode,[9] i.e., with the sample back surface–PVDF distance L large in comparison to the thermal diffusion length in the airgap between the two surfaces. This "infinite" distance condition could be satisfied in the thermally thick air layer for $L \geq 5$ mm at chopping frequency $f = 9$ Hz. At this "infinite" distance the quadrature of the lock-in amplifier was set equal to 0, in order to make the in-phase channel the sole detector of any directly transmitted optical energy flux through the sample, typically in the *a*-Si:H thin-film subgap region. Thermal energy transmission in the form of thermal waves was detected at each wavelength imme-

diately following the "infinite distance" purely optical measurement by decreasing the distance L to some predetermined value < 1 mm, where a measurable stable lock-in quadrature signal was present as a result of optical-to-thermal energy conversion in the sample and thermal-wave release in the airgap. Experimentally, the quadratures of the signals corresponding to "infinite" and "finite" L-distances were subtracted at each wavelength in order to cancel out photopyroelectric phase shifts induced by different dc optical heating levels of the polymer PVDF as the transmitted optical flux from the 1000-W Xe lamp varied with optical throughput throughout the spectral scan. In our experience, this operation must be adhered to with very weak thermal-wave sources such as the a-Si:H thin films of this study, especially in the near-IR sub-gap region where both Si substrates and deposited amorphous thin films are (at least partially) transparent and the optical flux directly transmitted to the PVDF detector can cause significant dc temperature fluctuations. These fluctuations, in turn, can generate signal-dominating instrumental phase shifts and must be compensated for by subtraction, if the full phase-resolution capability of PPES is to be utilized.

For the present study a few a-Si samples of thicknesses 500, 2100, and 8000 Å deposited on crystalline Si wafers were used. The samples were obtained from MITEL Semiconductors (Bromont, Quebec). The thin films were deposited at 570°C with MITEL's low-pressure chemical vapor deposition (LPCVD) process. Some investigations on these films have shown the presence of polycrystalline silicon. This observation is consistent with the fact that the relatively high deposition temperature is close to the critical one (670°C) where the formation of polycrystalline silicon occurs.[13] The samples themselves were cut in square shapes with dimensions of 4 × 4 mm² to fit onto the sample holder. The substrates were crystalline silicon wafers with nominal resistivities ranging between 2 and 4 Ω cm. In principle, a properly designed wafer holder allowing the positioning of entire wafers can be used with the present technique, thus eliminating the usual destructive necessity for cutting small samples to fit inside, for example, photoacoustic gas-microphone cells.

The PVDF active element was housed in a commercial Inficon® housing with the cap modified (thinned down) to allow as small an airgap as possible in case of unacceptably low signal-to-noise ratios (SNRs). The PVDF surface was sooted lightly in order to eliminate optical reflections and thus maximize the in-phase photopyroelectric signal levels, due to purely optical transmission through the sample bulk. The presence of the soot had little effect on the Q-PPES signal levels, in the sense that its micrometer-level thickness did not become the source of laterally inhomogeneous phase shifts across the PVDF surface as determined by scanning with a He–Ne laser beam. Such phase shifts are common in spray-painted PVDF because of the appreciably thicker paint layers (~200–300 μm)[5] and affect the quantitative reproducibility of data upon removal and repositioning of the PPE detector behind an optically excited, translucent, or transparent sample, such as the semiconductor materials investigated in this work, or quantum-well structures on GaAs substrates.[5] The distance L could be varied automatically by the IBM PS/2 computer controlling the experiment by virtue of a micrometer stage supporting the pyroelectric element assembly. Spectroscopic measurements were performed between 920 and 1500 nm at a chopping frequency of 9 Hz.

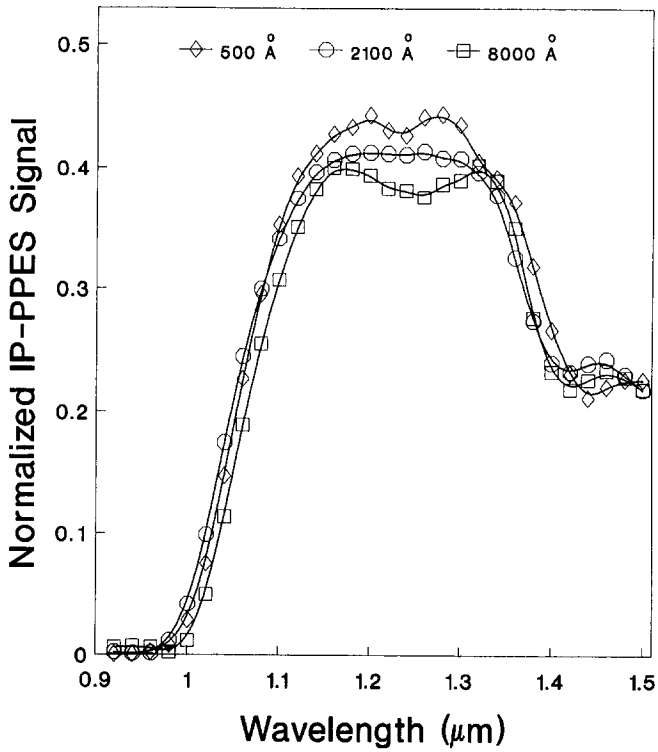

FIG. 2. Normalized IP-PPE (purely optical transmission) spectra of three a-Si:H thin-film samples deposited on crystalline Si oriented opposite from the incident radiation. Chopping frequency f = 9 Hz.

Optical transmittance and reflectance spectra in the same wavelength range were also obtained with a standard FT-IR spectrometer for comparison with the IP- and Q-PPE spectra.

RESULTS AND DISCUSSION

Photopyroelectric spectra were normalized by the lamp spectrum. They can be divided into IP (purely optical transmission), and Q (purely thermal-wave), spectra. Figure 2 shows results with the three amorphous thin-film layers oriented opposite from the incident light facing the PVDF detector, and the back, unpolished silicon wafer surface directed toward, and perpendicular to, the incident radiation. These spectra are typical photopyroelectric transmissions[3] exhibiting the expected sub-gap enhancement due to the increased transmitted power to the IP channel of the lock-in amplifier, as indicated in Eq. 2. Similar spectra are shown in Fig. 3, obtained with the sample orientation reversed. In both sets of spectra it is apparent that the resolution of the IP-PPES technique is inadequate to separate out transmissions from the 50-nm- and 210-nm-thin films. In the case where the thin film lies facing the incident beam (Fig. 3), the resolution is the poorest, with the spectra from these two thin-film samples being essentially identical within experimental error. A comparison between the relative magnitudes of the two sets of spectra shown in Figs. 2 and 3 shows that those obtained with the polished surface toward the incident light are somewhat smaller, as expected from the

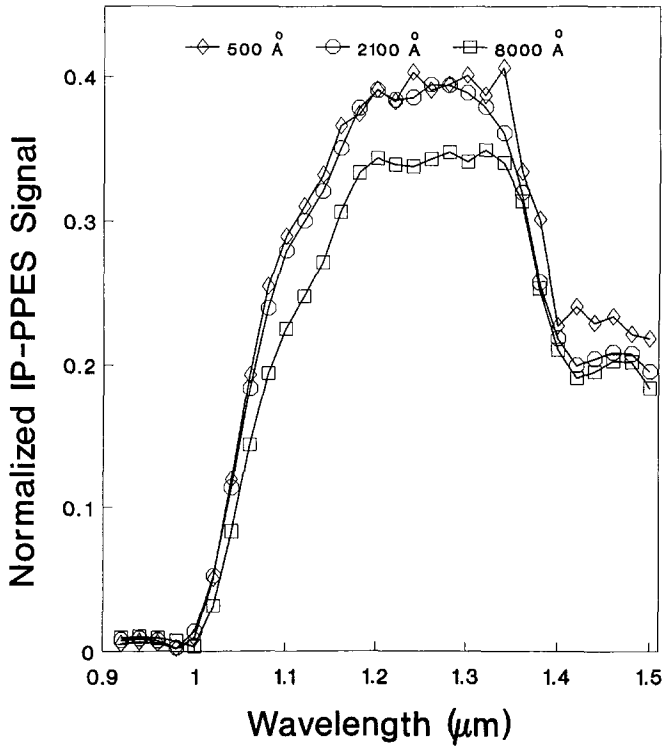

FIG. 3. Normalized IP-PPE (purely optical transmission) spectra of the three *a*-Si:H samples on crystalline Si oriented toward the incident radiation. Chopping frequency $f = 9$ Hz.

enhanced reflectance on the smooth surfaces. In both sets of spectra the one corresponding to the thickest (8000 Å) *a*-Si:H thin-film is of lower magnitude, as expected from the decreased optical transmission of the thickest layer. Nevertheless, the thin-film-thickness resolution of the IP-PPES transmission technique is seen to have a lower limit above the 2100-Å level.

FT-IR spectra of the wafers were also obtained for comparison with the samples placed on the surface of the photodiode detector of the spectrometer in order to minimize optical losses due to scattering events. Figure 4 shows the results both in reflection (Fig. 4A) and in transmission (Fig. 4B) with the polished surface of the samples toward the optical source. The opposite configuration did not yield measurable signals, because of the increased optical scattering. The 8000-Å thin-film reflectance spectrum is further seen to exhibit interference fringes. The order of spectral magnitude strength is not consistent between Figs. 4A and 4B, with the 8000-Å-thick layer producing a transmittance spectrum intermediate between the 500- and 2100-Å layers. This inconsistency, along with the discrepancies in spectral order between Fig. 4B and its PPE equivalent, Fig. 3, indicates the low resolution of the conventional FT-IR technique manifesting itself as the inability to yield quantitatively correct information on thin amorphous semiconducting layers deposited on substrate wafers. The poor resolution of the FT-IR spectra may further be responsible for their insensitivity to the spectral feature ("plateau") observed in the $\lambda > 1300$-nm region of Figs. 2 and 3. These spectral plateaus are tentatively assigned to impurity absorptions in the bulk of the substrate wafers and have also been detected in the IP-PPE spectrum of unprocessed Si wafers. The increased

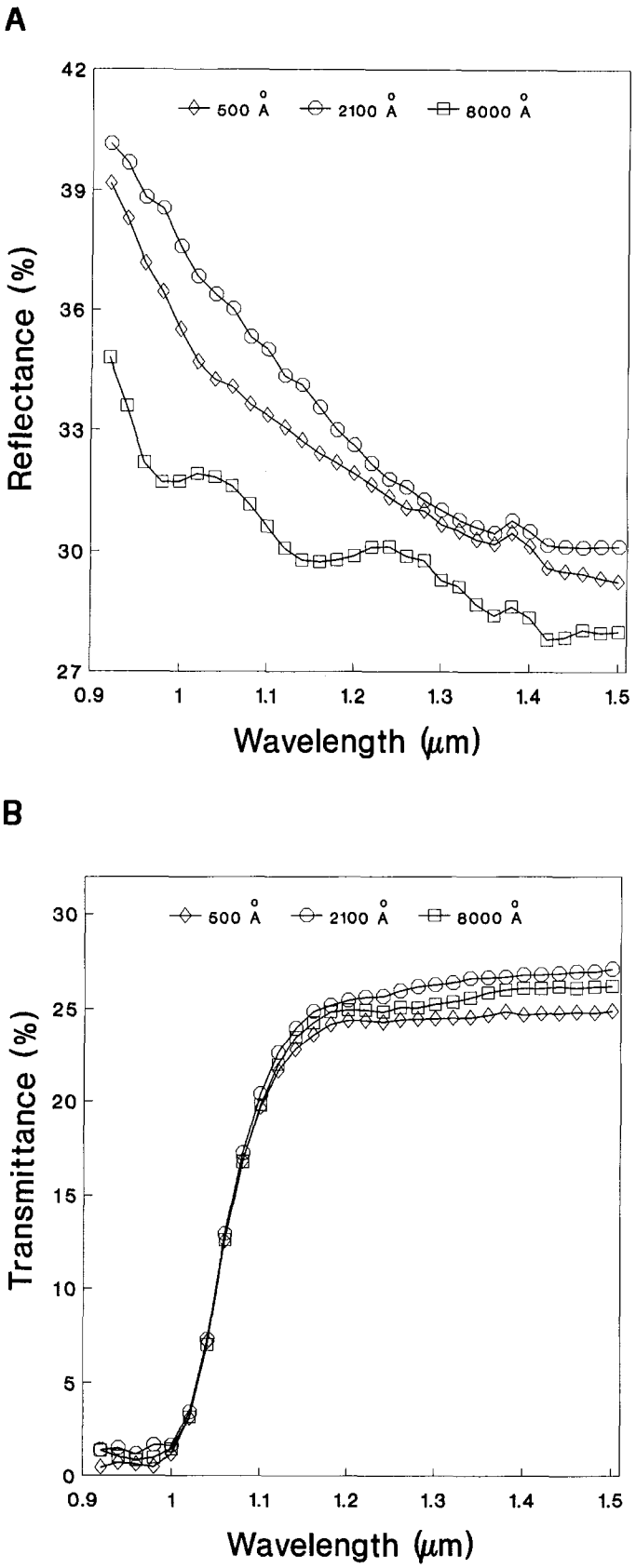

FIG. 4. (A) Reflectance and (B) transmittance FT-IR spectra of the three *a*-Si:H samples.

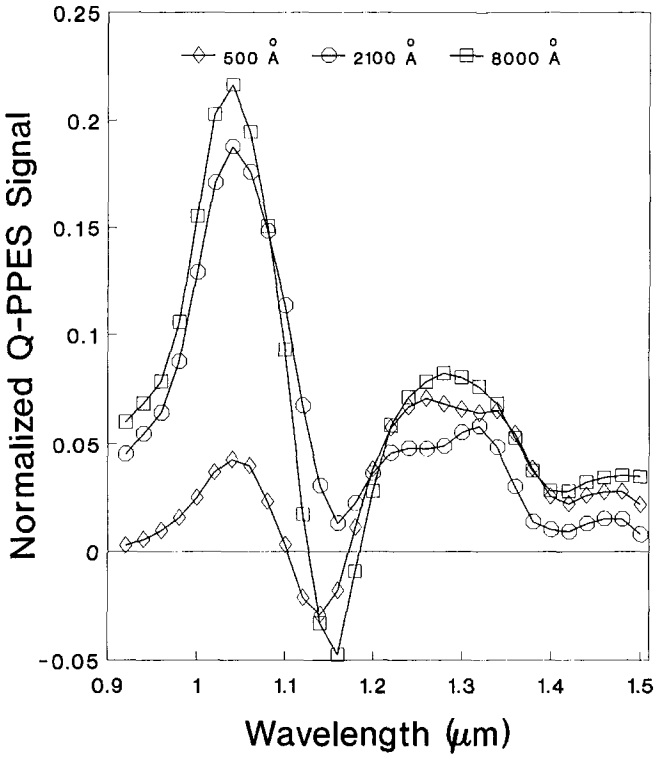

FIG. 5. Normalized Q-PPE (purely thermal-wave) spectra of the three *a*-Si:H thin-film samples oriented opposite from the incident radiation. Chopping frequency $f = 9$ Hz.

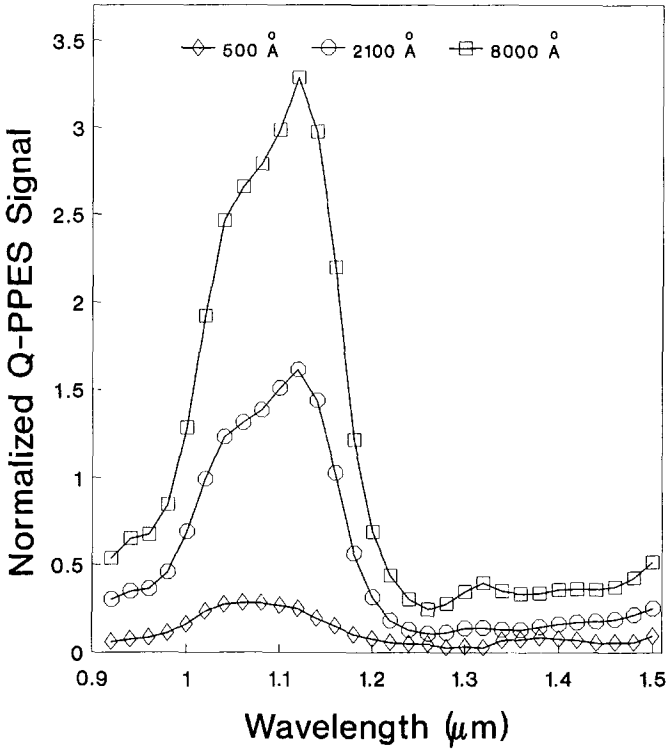

FIG. 6. Normalized Q-PPE (purely thermal-wave) spectra of the *a*-Si:H thin-film samples oriented toward the incident radiation. Chopping frequency $f = 9$ Hz.

sensitivity of the PPE detector acting as a transmission radiation collector can be understood by comparing the relatively very large active area of this detector (~ 0.5 cm^2) to that of the photodiode in the FT-IR spectrometer (~ 1 mm^2).

The Q-PPE spectra of the samples are shown in Figs. 5 and 6. These figures correspond to the configurations of Figs. 2 and 3, respectively. In the geometry of Fig. 5, where the thin-film *a*-Si:H surfaces of the sample wafers were placed within a thermal wavelength from the PVDF detector, one clearly sees the excellent resolution of the quadrature signals down to the minimum available 500-Å thickness and beyond. The main peaks at $\sim\lambda = 1$ μm scale with thin-film thickness and may contain optical interference contributions (especially the 8000-Å spectrum in view of Fig. 4A). This feature of the 8000-Å spectrum is probably responsible for the crossing of this spectral curve over the other two line shapes. Overall, the origin of the main peaks is not primarily interferometric, as might seem at first glance in the presence of spectrally oscillatory features, but is attributable to the interplay between enhanced optical intensity arriving at the absorbing thin-film layer just below the bandgap of the overlying substrate Si wafer and thus *increasing* the magnitude of thermal-wave signals, and the decrease in thin-film absorptance with increasing wavelength,[3] which tends to *decrease* the magnitude of the occluded thermal-wave signals. The oscillatory spectral features below $\lambda \sim 1.16$ μm are related to the plateaus observed in the IP (purely optical transmission) mode, Fig. 2, and can be explained in terms of nonradiative defect/impurity structures in the sub-gap region; the increased absorptance responsible for the spectral plateau of Fig. 2 is thus seen to give rise to enhanced thermal energy release which is responsible for the $\lambda > 1.16$ μm Q-PPES signal strength, as indicated in Eq. 3. The fact that all three spectral curves exhibit far lower relative resolution in this region than in the higher photon energy regime led to the conclusion that the main source of the nonradiative structures must be the underlying thermally thick silicon wafer bulk. Indeed, further experiments with a silicon wafer from the same batch but without the surface-deposited *a*-Si layers showed substantial sub-bandgap absorption features in the same spectral region. A logarithmic extrapolation down to zero absorptance of the peak magnitudes in the vicinity of $\lambda = 1$ μm in Fig. 5 gave an estimate of less than 100 ± 20 Å as the minimum detectable *a*-Si:H film thickness in that region.

When the Q-PPES spectra of Fig. 5 are compared with those of Fig. 6 obtained with the sample configuration which produced the spectra of Fig. 3, two major features become apparent: the dynamic range of the spectral resolution is much better in the 8000–500 Å range of thicknesses; and the effects of thin-film sub-gap and/or substrate sub-bandgap absorptions are much less pronounced when the thin film is oriented toward the light. This is the optimal mode for quantitative Q-PPES measurements, since the spectral order follows a strict sequence from the thicker to the thinner thin-film sample and no cross-overs are observed, even in the presence of some optical interference fringes (Fig. 4A). Despite the increased reflectance from the polished and thin-film deposited surface, the sensitivity of Fig. 6 in both relative (normalized signal) and absolute (signal magnitude) terms is higher than that of Fig. 5 by more than one order of magnitude.

The higher dynamic range of the spectral resolution in Fig. 6 can be explained if one considers that the entire strength of the optical fluence incident on the sample encounters the thin film first, which plays the primary role in its attenuation and the optical-to-thermal energy conversion. On the other hand, in the geometry of Fig. 5, the thin film can only receive a much diminished optical fluence because of the overlying Si wafer bulk and the sub-bandgap absorptions associated with it below 1.25 μm. This limitation appears to interfere with the ability of the detector element to optimally resolve the total thermal energy released in the backside thin film as distinct from that released in the vastly thicker (and absorbing) silicon overlayer, as described in Eq. 3. This factor, of course, has an impact on the ability of that particular geometry to optimally resolve the backside thin-film thickness, although the observed spectral resolution is much better than the one afforded by the conventional FT-IR technique.

In explaining the considerable signal improvement of Fig. 6 over that of Fig. 5, it must be kept in mind that both amorphous Si thin films *and* bulk nonradiative defects in substrate crystalline Si are efficient (~100%) optical-to-thermal energy conversion centers, with the former being a much more localized (surface) energy converter. In the geometry of Fig. 5 the nonradiative thermal-wave energy flux generated in the thin film at the backside is quite limited in magnitude because of the overlying and absorbing Si bulk. In the geometry of Fig. 6, however, given that at 9 Hz the samples are thermally thin,[12] the large-magnitude optically generated nonradiative thermal-wave flux in the thin surface films propagates essentially unattenuated to the backside of the wafer and then across to the PVDF detector surface via the airgap layer, where the thermal-wave attenuation is the same for both sample direction geometries. The relative PPE signal levels thus arising are quite strong because of the high fluence *and* efficient optical-to-thermal energy conversion at the front surface, along with the thermally thin condition. Theoretically, an analysis of the foregoing trends is possible, in principle, by determining the factors F_b and F_s in Eq. 3 for each orientation of the sample. In terms of the quadrature signal it is found that the effect of the thermal-wave contribution due to the nonradiative surface heat release diminishes by a factor of $\exp(-\beta\ell)$ in the geometry of Fig. 5 over that of the geometry of Fig. 6,[11] consistent with the decreased effect of the amorphous surface layers observed in Fig. 5. Further evidence of the amorphous surface thin-film origin of the large thermal-wave signal peaks in Fig. 6 is in the relative ratios of the peaks at $\sim\lambda = 1.1$ μm (more than $\times 15$ higher than the respective features in Fig. 5) and of the bulk-related sub-bandgap absorption levels at $\lambda > 1.25$ μm; these ratios are approximately 9.4 in Fig. 6 and only 2.5 in Fig. 5. On extrapolation from the peak signals of Fig. 6 down to zero signal level in a semi-logarithmic plot in a manner similar to the foregoing extrapolation performed with the peaks of Fig. 5, it was estimated that the minimum detectable *a*-Si:H thin-film thickness is 40 ± 20 Å.

CONCLUSION

Noncontacting, purely thermal-wave-mode Q-PPES was proven to be a photothermal technique quite suitable for the quantitative spectroscopic study of *a*-Si:H thin film deposited on top of crystalline Si wafers. This detection channel has exhibited much better performance than optical FT-IR detection in terms of thin-film thickness resolution and sensitivity to weak sub-bandgap absorptions in Si. Similar assessments were made in comparing Q-PPES with its IP-PPES counterpart with the use of the same PVDF detector acting like a purely optical sensor. Between the two possible sample positioning geometries under thermally thin conditions (one with the polished and thin-film-deposited surface toward the incident radiation, and the other with the reverse geometry), the former configuration was shown to produce higher thin-film spectral resolution (dynamic range) and more than one order of magnitude stronger photothermal signals, consistent with qualitative theoretical considerations of the Q-PPES signal. As a result, the extrapolated minimum mean detectable *a*-Si:H thin-film thicknesses are 40 Å for the former sample positioning configuration and 100 Å for the latter.

ACKNOWLEDGMENT

The authors gratefully acknowledge a Strategic Grant from the Natural Sciences and Engineering Research Council of Canada (NSERC), which made the development of the noncontact Q-PPES technique and this work possible.

1. A. Mandelis, R. E. Wagner, K. Ghandi, R. Baltman, and P. Dao, Phys. Rev.B **39,** 5254 (1989).
2. C. Christofides, A. Mandelis, and K. Ghandi, Rev. Sci. Instrum. **61,** 2360 (1990).
3. C. Christofides, A. Engel, and A. Mandelis, Ferroelectrics **118,** 411 (1991).
4. C. Christofides, A. Mandelis, A. Engel, M. Bisson, and G. Harling, Can. J. Phys. **69,** 317 (1991).
5. A. Mandelis and A. da Silva, Ferroelectrics, paper in press.
6. J. Fan and J. Kakalios, Phil Mag. Lett. **64,** 235 (1991).
7. J. Fan and J. Kakalios, M.R.S. Conf. Proc. **219,** 545 (1991).
8. H. Coufal, Appl. Phys. Lett. **45,** 516 (1984).
9. A. Mandelis, J. Vanniasinkam, S. Buddhudu, A. Othonos, and M. Kokta, Phys. Rev. B **48,** 6808 (1993).
10. S. Buddhudu, J. Vanniasinkam, A. Mandelis, B. Joseph, and K. Fjeldsted, Opt. Mater. **3,** 115 (1994).
11. J. Vanniasinkam, A. Mandelis, S. Buddhudu, and M. Kokta, J. Appl. Phys. **75,** 8090 (1994).
12. A. Mandelis and M. M. Zver, J. Appl. Phys. **57,** 4421 (1985).
13. P. J. Zanzucchi, C. R. Wronski, and D. E. Carlson, J. Appl. Phys. **48,** 5227 (1977).